Modelling of Spatial Synchrony in Acorn Masting for Ecosystem Management

Takahiro Yamazaki[†,‡] and Kenshi Sakai[†*]

† Department of Environmental and Agricultural Engineering, Tokyo University of Agriculture and Technology
Remote Sensing Technology Center in Japan (at Present)
Saiwai-cho,Fuchu-shi,Tokyo 183-8509,Japan
‡ Remote Sensing Technology Center of Japan
TOKYU REIT Toranomon Building 3F 3-17-1 Toranomon, Minato - ku, Tokyo 105 - 0001, Japan
Email: t.zakiyama1015@gmail.com, *corresponding author Email: ken@cc.tuat.ac.jp

1.Introduction

Masting (mast seeding) is a phenomenon in which acorn production alternates between large and small yields over years (Kelly 1994). Masting is recognized as an important process for both wild-life management and natural regeneration in secondary forests. Large fluctuations in the acorn production of individual trees are due to nonlinear dynamics described as a tent map with y-intercept (Isagi,1996,Sakai 2001), and spatial synchrony is also caused by pollen coupling between trees. The spatiotemporal dynamics of masting is important from the point of ecosystem management and theoretical ecology.

In this paper, we developed a GIS-based mating modeling technique. Individual canopies were identified through airborne image segmentation, and essential data for each canopy, such as location and size, were measured in the segmentation process. Our model is based on the concept of a coupled map lattice. The dynamics of the acorn production of each tree is modeled as an oscillator in the CML. Coupling in this CML corresponds to pollen coupling between trees. To determine the features of the developed spatiotemporal dynamics, we employed a spatial autocorrelation function and conducted a parameter study by changing fundamental system parameters such as coupling strength. The output of the model was expressed in a GIS base to enable easy visualization of the spatiotemporal dynamics and spatial synchrony.

2. Material and Method

2.1 Study site

We obtained airborne images of the forest experimental stations of Tokyo University of Agriculture and Technilogi located at 35°38’18”N, E139°22’41”. The site is 38 ha and the predominant species is *Quercus serrata*. The image in Fig.1 was taken on May 26, 2004, and multi-spectral imaging at a spatial resolution of 0.2m/pixel was employed.

Fig.1 Airborne image of the study site

2.2 Extraction of canopies

Segmentation was used to extract each canopy using the image processing system eCognition™. The segmentation process is shown in Fig. 2. The first segmentation step separated the vegetation and urban areas. In this process, we set the scale parameter as 1000, color/shape = 9:1, and compactness/ smoothness = 1:1. Additionally, we identified broadleaf trees from conifer, grassland, buildings and roads via the edit tool of eCognition™ (Fig. 2b). In the next process, we set the scale parameter as 30, color/shape = 1:1, and compactness/smoothness = 7:3, which facilitated the extraction of 6267 canopies (Fig. 2c). The canopy objects obtained were exported in shp file format for expression in GIS. The shp file contained object ID, area (m^2), CG latitude and longitude, shape index and mean RGB. Via AceGIS 10.01, we eliminated noise, shadow and anomalies, and obtained 4703 objects (Fig.2d). The *shape index* was defined as,

$$shape\_index = \frac{Length}{4\sqrt{Area}}$$

to identify sufficiently long objects as tree canopies.

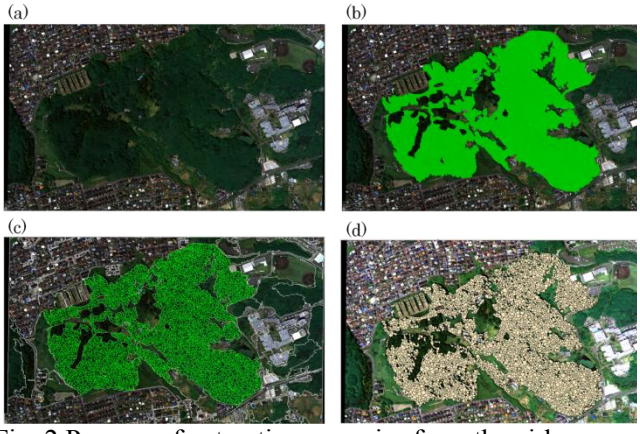

Fig. 2 Process of extracting canopies from the airborne multispectral image. a, **A**irborne multispectral image; b, Forest objects; c, Row canopy objects; d, Canopy objects identified as *Quercus serrata*.

3. GIS-based masting model

3.1. Photosynthate P_S and Threshold L_T

The masting model was based on Isagi's resource budget model (RBM) (Isagi 1996, Sakai, 2001; Satake & Iwasa, 2002). In most previous studies, an endogenous mechanism was proposed to explain the masting of an individual tree and the synchrony of masting in a forest; thus, parameters such as Photosynthate P_S and Threshold L_T were assumed to be homogenous.

In this paper, we were interested in the effect of the distribution of canopy size on masting and on masting synchrony; therefore, we set Photosynthate P_S as equal and Threshold L_T as proportional to each tree (canopy) area, respectively.

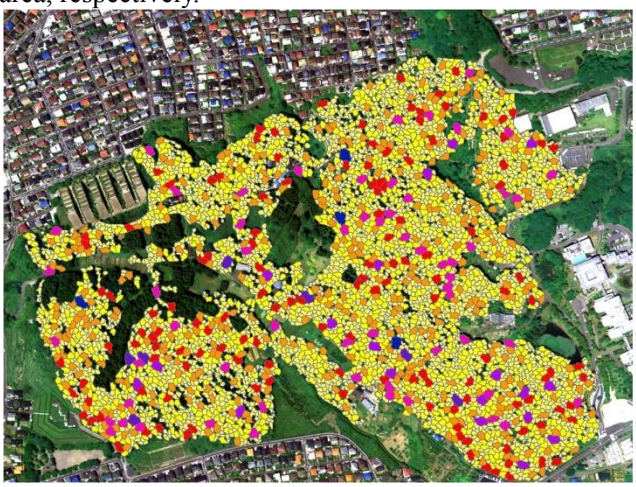

Fig. 3 Spatial distribution of Photosynthate P_S

Fig. 3 shows the spatial distribution of P_S, and L_T is defined as $L_T{}^i = R_C P_S{}^i$.

3.2. Model

The CML of RBM (Satake&Swasa, 2002) modeled pollen distribution density as constant within a given area. For anemophilous plants, however, pollen distribution density is reported to decline with increasing distance from the tree (Austerlitz et al. 2004). Therefore, we developed a pollen density matrix **P** in which the element $p^{i,j}$ denotes the pollen density at location i from a tree located at j.

$$\mathbf{P} = \begin{pmatrix} p^{1,1} & \cdots & p^{1,j} & \cdots & p^{1,n} \\ \vdots & \ddots & & & \vdots \\ p^{i,1} & & p^{i,j} & & p^{i,n} \\ \vdots & & & \ddots & \vdots \\ p^{n,1} & \cdots & p^{n,j} & \cdots & p^{n,n} \end{pmatrix} \quad (1)$$

where、

$$p^{i,j} = \frac{1}{\sqrt{2\pi\sigma^2}} \exp\left[-\left(\frac{d^{i,j}}{\sqrt{2}\sigma} \right)^2 \right] \quad (2)$$

$$d^{i,j} = \sqrt{\left(x^i - x^j\right)^2 + \left(y^i - y^j\right)^2} \quad (3)$$

where $p^{i,j}$ is defined as a 2-dimensional normal distribution function. $d^{i,j}$ is the distance between tree i and j, and x and y are its latitude and longitude, respectively. Here, we call $p^{i,j}$ the pollen kernel (Fig. 4).

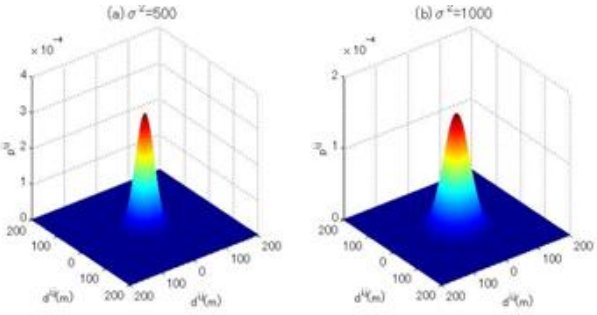

Fig. 4. Pollen kernel

We define the pollination rate of tree i, $X^i(t)$, as a logistic function:

$$X^i(t) = \frac{1}{1 + k\exp\left(-l\sum_{j=1}^{n} p^{i,j} C_f{}^j(t) \right)} \quad (4)$$

where the term $\sum_{j=1}^{n} p^{i,j} C_f{}^j(t)$ is the total amount of pollen supplied from tree j to tree i. As shown in Fig. 5, the parameters k and l of the pollination ratio $X^i(t)$

indicate the *y* intercept and coupling strength**,** which are denoted α in Isagi's model (Isagi 1996).

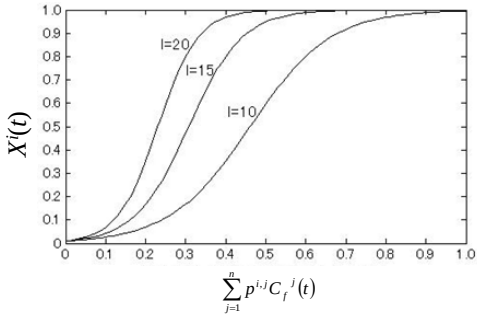

Fig.5. Pollination ratio $X^i(t)$
k=100

Using the newly defined phtosynthate $P_S{}^i$, threshold $L_T{}^i$, and pollination ratio $X^i(t)$, our model is described as follows**:**

$$S^i(t+1)=\begin{cases} S^i(t)+P_S{}^i & \text{if} \quad S^i(t)+P_S{}^i \le L_T \\ S^i(t)+P_S{}^i-C_f{}^i(t)-C_a{}^i(t) & \text{if} \quad S^i(t)+P_S{}^i > L_T \end{cases} \tag{5}$$

$$C_f{}^i(t)=S^i(t)+P_S{}^i-L_T{}^i \tag{6}$$

$$C_a{}^i(t)=R_C C_f{}^i(t) X^i(t) \tag{7}$$

where, $S(t)$:energy reserves of plant at the beginning of year t. $C_f(t)$:the cost of flowering. $C_a(t)$:the cost of fruiting. $R_C=C_a/C_f$.

4. Numerical experiments

4.1. Parameter setting

The number of canopy objects was 4703**.** Numerical experiments were conducted for 18 parameter combination**s** consisting of R_C=1.5, 2.5**;** k=100, l=10, 15, 20; σ^2= 500, 1000, 2000. Phtosynthate $P_S{}^i$ values as shown in Fig. 3 were used and the average of them was calculated as 55.4639.

The initial values of the accumulated resource**,** $S^i(0)$**,** were given as uniform random values from 0 to $L_T{}^i$. A 100-year time series of matured seeds cost $C_a{}^i(t)$ data after 10000 years of iterations were used in the analysis to avoid transient states.

4.2. Results

As one example, the spatial distributions of acorn production for one of the 18 parameter combinations are shown in Fig.6. A 2-year period can be observed; in addition, the on trees and off trees also can be seen within each year.

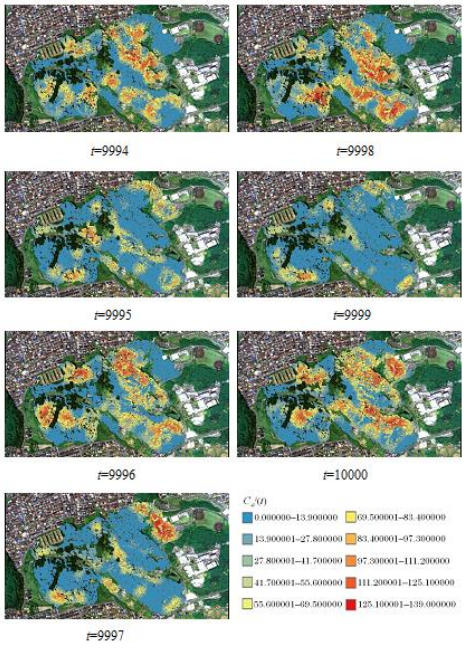

Fig.6 Spatio-temporal dynamics under R_C=2.5, l=10, σ^2=1000, $P_S{}^i$=55.4639

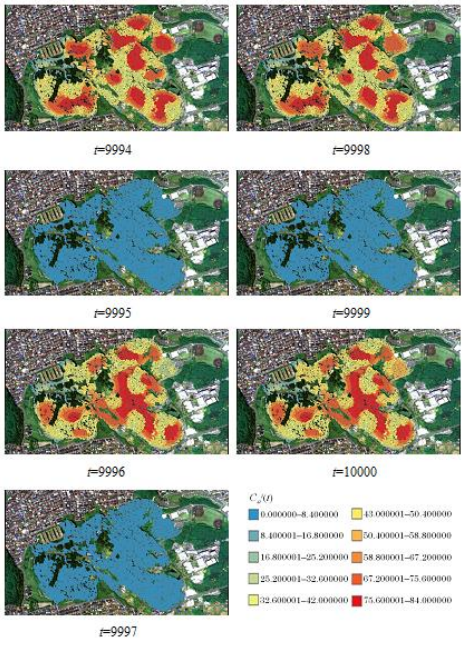

Fig. 7 Spatio-temporal dynamics under R_C=1.5, l=10, σ^2=1000, $P_S{}^i$=55.46398(4.23)

4.3. Spatial correlation

We employed Moran's I and Spatial Pearson's correlation function to evaluate the results of the numerical experiments (Akita et al., 2008; Rosenstock et al., 2011) as shown in Fig.8.

Moran's I**:**

$$r(lag)=\frac{n}{W(lag)}\frac{\sum_{i=1}^{n}\sum_{j=1}^{n}w^{i,j}(lag)\left(z^i(t)-\overline{z^i(t)}\right)\left(z^j(t)-\overline{z^i(t)}\right)}{\sum_{i=1}^{n}\left(z^i(t)-\overline{z^i(t)}\right)^2} \quad (8)$$

Spatial Pearson's correlation function:

$$\rho(lag)=\frac{1}{W(lag)}\sum_{i=1}^{n}\sum_{j\neq i}^{n}w^{i,j}(lag)\upsilon\left(z^i(t),z^j(t)\right) \quad (9)$$

where,

$$\upsilon\left(z^i(t),z^j(t)\right)=\frac{\frac{1}{T}\sum_{t=1}^{T}\left(z^i(t)-\overline{z^i(t)}\right)\left(z^j(t)-\overline{z^j(t)}\right)}{std\left(z^i(t),\overline{z^i(t)}\right)std\left(z^j(t),\overline{z^j(t)}\right)},$$

$$std\left(z^i(t),\overline{z^i(t)}\right)=\sqrt{\frac{\sum_{t=1}^{T}\left(z^i(t)-\overline{z^i(t)}\right)^2}{T}}$$

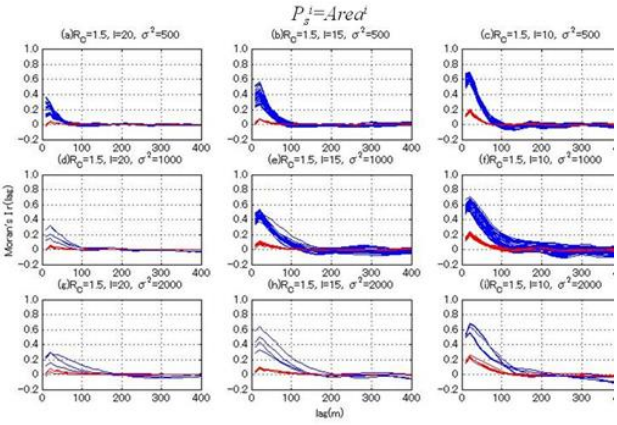

Fig.8 Moran's I$r(lag)$ for matured seed costs $C_a^i(t)$. Red, on years tree**;** blue, off years tree; $P_S^i = Area^i$, R_C=1.5

4.4. Index of synchrony

The individual coefficient variance CV_i, correlation coefficient between individual trees ρ**,** and population coefficient of variance CV_p were calculated (Tables 1 and 2). Additionally, we defined the year coefficient variance CV_y as

$$CV_y=\frac{1}{T}\sum_{t=1}^{T}\frac{std\left(z^i(t),Z(t)\right)}{Z(t)} \quad (10)$$

where $Z(t)=\frac{1}{n}\sum_{i=1}^{n}z^i(t)$, $std\left(z^i(t),Z(t)\right)=\sqrt{\frac{\sum_{i=1}^{n}\left(z^i(t)-Z(t)\right)^2}{n}}$

Table1 CV_i,CV_p,CV_y and ρ ;P_S^i=$Area^i$、R_C=2.5

P_S	R_C	l	σ^2	CV_i	CV_p	CV_y	ρ
$Area^i$	1.5	20	500	1.0687	0.9857	1.0848	0.8511
			1000	1.0686	0.9884	1.1092	0.8568
			2000	1.0692	0.9906	1.1049	0.8539
		15	500	1.0637	0.9878	1.3049	0.86
			1000	1.0599	0.9922	1.2287	0.8741
			2000	1.0573	0.9875	1.2752	0.8707
		10	500	1.0258	0.9779	1.4464	0.8919
			1000	1.0165	0.9765	1.3435	0.9036
			2000	1.0032	0.9758	1.3851	0.9183

Table2 CV_i,CV_p,CV_y and ρ, P_S^i=55.4639、R_C=1.5

P_S	R_C	l	σ^2	CV_i	CV_p	CV_y	ρ
$Area^i$	2.5	20	500	1.0968	0.1001	1.4277	0.0081
			1000	1.066	0.1145	1.3874	0.0113
			2000	1.0447	0.1854	1.363	0.0328
		15	500	1.0625	0.0934	1.3945	0.0071
			1000	1.0522	0.1909	1.3759	0.0317
			2000	1.0463	0.2394	1.3764	0.0505
		10	500	1.0307	0.1413	1.4015	0.0177
			1000	1.0262	0.1791	1.3981	0.0294
			2000	0.9924	0.2312	1.3786	0.0459

5. Conclusions

The synchrony of acorn production was investigated via a GIS-based resource budget model**,** which is expected to predict acorn production at least one year in advance to aid wild-life animal management, vegetation management**,** and sustainable and low cost second forest management. The strength of pollen coupling is a key control parameter to govern the statio-temporal dynamics of masting synchrony. In practice, information about pollen distribution at the landscape level is crucial to realize this attempt.

References

Akita T, Sakai K, Iwabuchi Y, Hoshino Y, Ye X (2008) Spatial autocorrelation in masting phenomena of Quercus serrata detected by multi-spectral imaging. Ecological Modelling, 215:217-224

Austerlitz F, Dick CW, Dutech C, Klein EK, Oddou-Muratorio S, Smouse PE, Sork VL (2004) Using genetic markers to estimate the pollen dispersal curve. Molecular Ecology, 13;937-954

Isagi Y, Sugiyama K, Sumida A, Ito H (1997) How does masting happen and synchronize?. Journal of Theoretical Biology, 187;231-239

Kelly D (1994) The evolutionary ecology of mast seeding. Trends Ecology and Evolution, 9;465-470

Rosen tock TS, Hastings A, Koenig WD, Lyles DJ, Brown PH (2011) Testing Moran's theorem in an agroecosystem, Oikos, 120;1434-1440

Satake A Iwasa Y (2002) Spatially Limited Pollen Exchange and a Long-Range Synchronization of Trees. Ecology, 83:993-1005

Sakai K (2001) Nonlinear Dynamics in Alternate Bearing and Masting of Tree Crops. In: Sakai K, Nonlinear Dynamics and Chaos in Agricultural Systems, 59-77. Elsevier Science B.V., Netherlands

Sakai,K.,Noguchi,Y.Asada,S. ,(2008) Detecting Chaos in a Citrus Orchard, Chaos Solitons and Fractals, 38(5),1274-1282

Acknowledgement

This project was financially supported by JSPS Grant-in aid No. 40192083